SECOND BREAKDOWN IN POWER TRANSISTORS DUE TO AVALANCHE INJECTION

Brent A. Beatty, Surinder Krishna and Michael S. Adler

ABSTRACT

This paper studies the subject of reverse bias second breakdown both experimentally and analytically. It is seen that there is excellent correlation between theory and experiment. The conclusion of this investigation is that avalanche injection is the triggering mechanism. Further, the filamentary currents that result from this can in most cases result in device failure. It is also concluded that under fixed circuit conditions, the reverse bias second breakdown potential of a transistor is completely specified by the single parameter, V_p, which is the voltage necessary for avalanche injection.

NOTATION

D_n	diffusion coefficient of electrons, cm^2/sec
E	electric field intensity, volt/cm
G	ratio of the emitter to base current
i_b	lateral base current, amps
I_{B1}	positive base current during on time, amps
I_{B2}	negative base current during turn off time, amps
I_e	terminal emitter current, amps
I_c	terminal collector current, amps
$j_e(x)$	lateral emitter current density, $amps/cm^2$
J_{max}	maximum emitter current density, $amps/cm^2$
k	Boltzmann's constant, eV/°k
L	inductance, henrys
$n_e(x)$	injected electron concentration, cm^{-3}
n_i	intrinsic electron concentration, cm^{-3}
N_{BO}	base impurity surface concentration under emitter, cm^{-3}
N_{EO}	emitter impurity surface concentration, cm^{-3}
N_C	collector impurity concentration, cm^{-3}
q	electron charge, coulombs
T	absolute temperature, °k
τ_d	delay time of pulse, sec
v_d	carrier drift velocity, cm/sec
v_l	carrier scatter limited velocity, cm/sec
V(x)	lateral voltage drop, volt
V_{CBO}	collector-base breakdown voltage, volts
V_p	collector voltage necessary for second breakdown, volts
W_B	metallurgical base width, cm
$W_B(x,y)$	metallurgical and induced base width, cm
W_C	collector width, cm
W_E	emitter junction depth, cm
Z	total emitter stripe length, cm
$\sigma(x)$	conductivity of the base, mho/cm
$\sigma_1(x)$	modulated conductivity of the base, mho/cm
σ_0	unmodulated conductivity of base, mho/cm
μ_{eff}	weighted average mobility of electrons and holes in base, $cm^2/volt\text{-}sec$
ε	dielectric constant, farads/cm

This paper was presented at the 1976 Power Electronics Specialists Conference, June 10, 1976.

The authors are with Corporate Research and Development, General Electric Company, Schenectady, New York.

INTRODUCTION

It has been seventeen years since Thorton and Simmons [1] first published a theory to explain the phenomenological failure of power transistors. Later there was speculation that the same destructive mechanism was responsible for failure in a variety of devices such as p-n junctions, point constant diodes, n^+-n-n^+ structures, and MOS transistors. The term second breakdown is used to describe a failure that is preceded by a precipitous drop in the voltage across the device and a rapid increase in current. Over the years several theories have been proposed to explain second breakdown [2]-[14]. However with further investigation, only three theories remain. The first is a mechanism that is associated with forward biased second breakdown and was proposed by Scarlett and Shockley [4]. Under these conditions, device failure resulted from a lateral thermal instability that was followed by a thermal runaway condition. The two other theories attempt to explain reverse biased second breakdown and may be termed as the "avalanche initiation" [6], [7] and the "thermal initiation" [13], [14] processes. It will be shown in this study that the avalanche process is the cause, and the thermal mechanism may well be the effect produced during second breakdown.

In order to determine the process that is responsible for failure, a priori choice is made between the contending theories. This was done by both Sunshine et al. [13] and Smith et al. [14]. The authors set out to detect hot filaments and found them present. The investigation, therefore, established a priori that a thermal process was responsible. In a similar vein this paper assumes the "avalanche process" is the cause of second breakdown. This study consists of an analysis of the mechanism supported by accurate experimental data. It may be pointed out that although a first order quantitative solution was given by Krishna et al. [7], both the analysis and the measurements were not quite accurate, and the results were, therefore, open to question. It has been the recent development of a sophisticated experimental circuit [15] that has resulted in accurate measurements. Also, a more exact analytical solution, based on a few valid assumptions, is responsible for the confidence in this model.

ANALYSIS

The sequence of events that occur in reverse bias second breakdown are the following: The lateral base current produces a voltage drop across the emitter base junction. This has the effect of constricting the current to the center of the emitter stripe, while back biasing the periphery. As the collector (and emitter) currents are held constant, the constriction causes a rapid increase in the emitter-collector current density.

If the concentration of the space charge entering the collector exceeds the fixed thermally ionized impurity concentration the mobile charge will determine the electric field in this region. If a voltage were applied

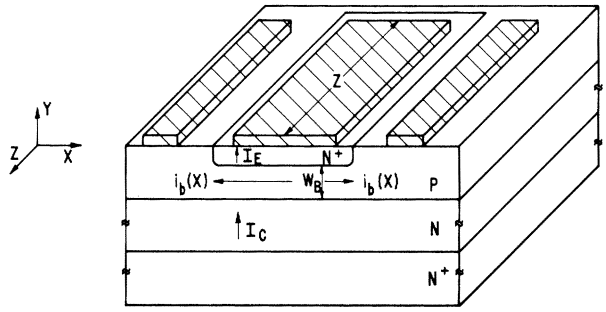

Fig. 1 Cross Section of a n^+-p-n -n^+ Transistor Showing Current Flow

in the presence of the space charge limited current, a situation can develop where the electric field exceeds its critical value for impact ionization. Multiplication and localized avalanche breakdown occurs. The resulting carriers produced in this region can give rise to current filaments. This aspect of the phenomena will be discussed in detail in a later section. For the purpose of the analysis, however, it is sufficient to calculate the "pinch in" current density in the emitter, and study the effects of this space charge in a collector region that must simultaneously support a high voltage. Fig. 1 shows the cross section of a transistor. The impurity distribution of the device is shown in Fig. 2. The diffusion profile and the geometric properties of the device influence the distribution of current density as follows:

The lateral current in the base per unit length of emitter is given by the expression

$$\frac{di_b}{dx} = \frac{1}{G} j_e(x) \tag{1}$$

The lateral voltage per unit length is

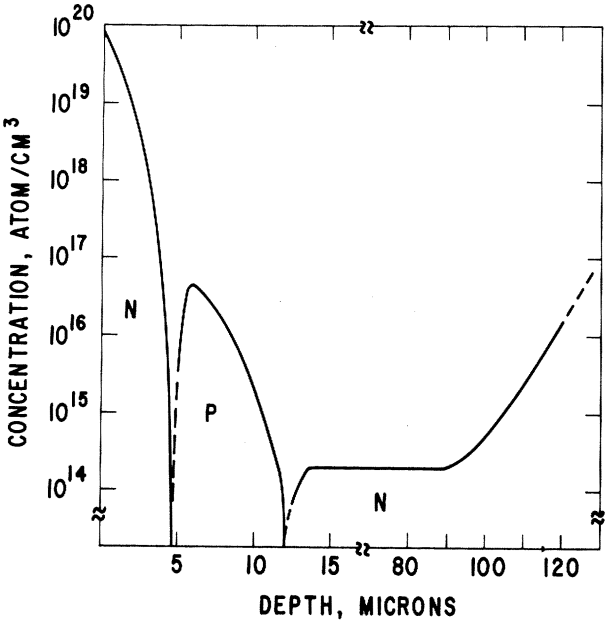

Fig. 2 A Spreading Resistance Profile Showing the Emitter, Base, and Collector Concentrations Versus Junction Depths

$$\frac{dV(x)}{dx} = -\frac{1}{W_B(x,y)} \cdot \frac{1}{\sigma(x)} i_b(x) \tag{2}$$

The conductivity $\sigma(x)$ consists of an unmodulated component σ_0 and a modulated component $\sigma_1(x)$. Under high injection conditions $\sigma_1(x)$ can be shown to be (see APPENDIX)

$$\sigma_1(x) = \frac{2}{3} \cdot q\mu_{eff} n_e(x) \tag{3}$$

Where under low injection conditions

$$n_e(x) = \frac{n_i^2}{N_{BO}} \cdot \exp \frac{qV(x)}{kT}, \qquad \text{if } n_e(x) \leq N_{BO} \tag{4}$$

TABLE II

Device #7

I_C AMPS	CALCULATED J_{MAX} AMPS/CM^2	CALCULATED V_P VOLTS	MEASURED V_P VOLTS
5	505	$> V_{CBO}$	V_{CBO}
10	755	715	680
12	836	635	600

At high injection levels

$$n_e(x) = n_i \exp \frac{qV(x)}{2kT}, \qquad \text{if } n_e(x) > N_{BO} \tag{5}$$

The emitter current density may then be expressed as

$$j_e(x) = \frac{qD_n}{W_B(x,y)} \cdot n_e(x) \left[1 + \frac{n_e(x)}{N_{BO} + n_e(x)}\right] \tag{6}$$

The terminal emitter current must, therefore, be related to (6) by the expression

$$I_e = 2Z \int_0^{\delta} j_e(x)dx, \qquad V(\delta) = \frac{2kT}{q} \tag{7}$$

Eqs. (1)-(7) are solved by the Runge-Kutta solution under the boundary condition at $x = 0$, $dV(x)/dx = 0$, $V = V(0)$ giving the following output:

(a) distribution of emitter current density along the stripe width as seen in Fig. 3, and its maximum value J_{max}

(b) the emitter base voltage developed across the junction

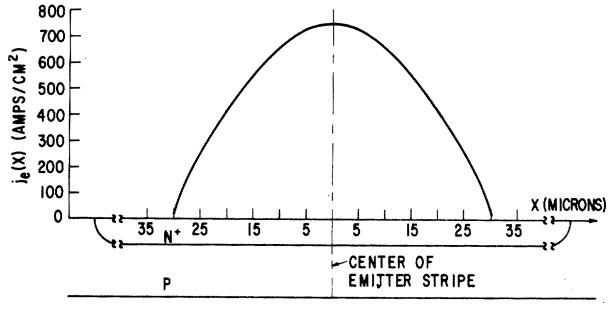

Fig. 3 Distribution of Current Density Along the Emitter Stripe

TABLE I

DEVICE #	N_{EO} ATOMS/CC	W_E MICRONS	N_{BO} ATOMS/CC	W_B MICRONS	N_C ATOMS/CC	W_C MICRONS	V_{CBO} VOLTS	CALCULATED J_{MAX} AMPS/CM^2	CALCULATED V_P VOLTS	MEASURED V_P VOLTS
1	6.1×10^{19}	5.5	5.2×10^{16}	7.0	2.0×10^{14}	44	660	809	620	620
2	6.5×10^{19}	6.13	2.4×10^{16}	7.13	2.8×10^{14}	42	680	784	650	550
3	6.0×10^{19}	5.6	5.3×10^{16}	7.25	2.0×10^{14}	46	700	783	640	620
4	6.5×10^{19}	5.6	3.0×10^{16}	7.38	2.3×10^{14}	40	650	752	640	550
5	4.0×10^{19}	5.13	2.3×10^{16}	6.75	2.0×10^{14}	67	1000	669	810	750
6	6.0×10^{19}	4.25	4.6×10^{16}	6.25	2.2×10^{14}	80	900	641	925	888
7	5.0×10^{19}	5.13	3.0×10^{16}	7.38	2.2×10^{14}	54	700	755	715	680

NOTE: IC = 10A

$$I_{B1} = I_{B2} = 1A$$

It is necessary to calculate (b) to verify that the emitter-base junction is not biased to the avalanche breakdown voltage V_{EBO}. Therefore, all the base current is through the base resistance, resulting in the emitter base potential along the stripe.

The maximum current density from the above solution is then included in Poisson's equation

$$\frac{dE}{dy} = \frac{q}{\varepsilon}\left(N_C - \frac{J_{max}}{qv_1}\right) \tag{8}$$

The drift velocity is always scattered limited in the case studied. This was independently determined by an exact solution of the current transport, continuity, and Poisson's equation. Therefore, $v_d \rightarrow v_1$ is a valid assumption. The solution of (8) gives the distribution of electric field in the collector. It is shown in Fig. 4 that the current density and fixed donor charge in the collector determine the slope, and along with the voltage, the maximum field. The solution of (8) gives the maximum voltage V_p for avalanche breakdown to occur. This is carried out by calculating the multiplication factor from the electron, hole ionization coefficients, and the electric field. For this analysis the values of Van Overstraeten [18] have been used. It is the voltage V_p that is necessary for the initiation of second breakdown. This calculated voltage is compared to the experimental value and will be seen in a later section to correlate very well. As this voltage V_p is unambituous and for a given device is determined from circuit conditions only, it expressed unequivocally the second breakdown capability of the transistor.

It should be pointed out that the equations for lateral base voltage V(x) and the collector voltage V(y) are interdependent by the term $W_B(x,y)$. It is this case width that ensures the solution of eqs. (1)-(7) and that of eq. (8) is self-consistent.

In some cases it was found that $W_B(x,y)$ was greater than the metallurgical base width. This suggests a "current induced base" exists in the presence of high voltages. Hitherto [16], the current induced base has been associated with low voltages present in the quasi saturation region of a transistor. This "current induced base" is present when the transistor is supporting the full voltage and load current. In the event the device has not reached the threshold V_p, for breakdown to occur, part of the fall time of the collector current may be determined by this expanded base width. This will happen only during the interval the time constant associated with the base width is greater than the circuit time constant given by the expression

$$I_c = -\frac{[V_{CE} - V_{CC}]}{L} \cdot t$$

V_{CE} is the voltage excursion of the device, and V_{CC} is the supply voltage in the collector circuit.

EXPERIMENTAL METHODS

Because of the catastrophic failure that generally accompanies reverse bias second breakdown, it is difficult to speculate that circuit parameters affects its initiation as the evidence is destroyed with the device. To solve this problem, a sophisticated circuit was designed and built that would force the device into a second breakdown and then sense the exact time of the

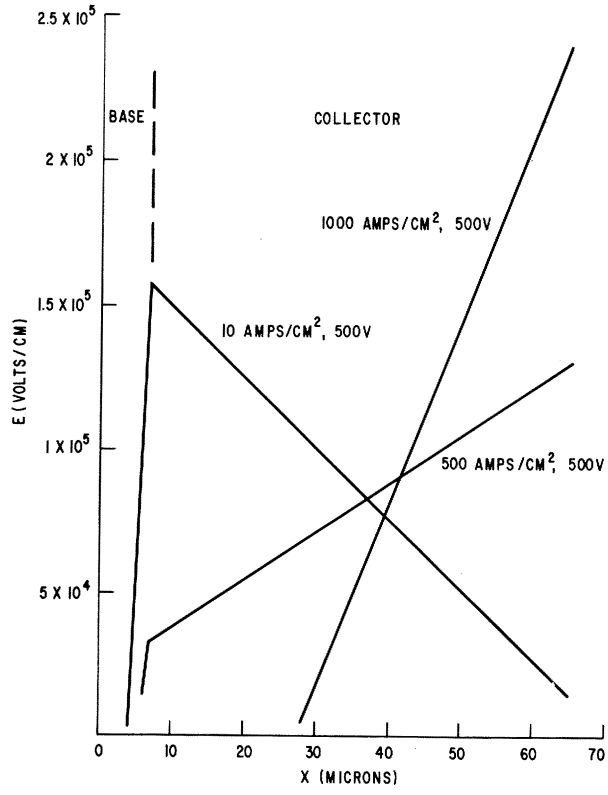

Fig. 4 Distribution of the Electric Field in the Collector for Different Current Densities

occurrence. After a prescribed delay the circuit applies a crowbar across the device which diverts the energy in the coil from the device. This circuit was designed and developed [15] for versatility and accuracy.

With this circuit, a transistor may be forced into second breakdown, and the destructive mechanism stopped before device degradation occurs. Circuits that have hitherto been proposed for measuring the second breakdown and safe operating regions [17] have lacked the capability of holding the input parameters constant

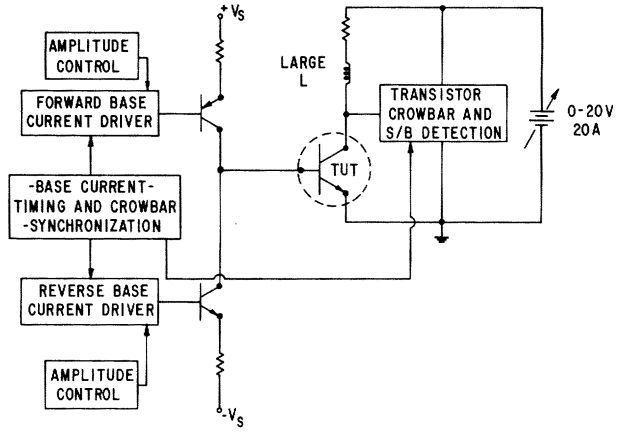

Fig. 5 Block Diagram of the Circuit Used in the Experiment

during the test or of protecting the device. For the purposes of this study, the input parameters are the exact conditions of the collector current and voltage. Also, the exact reverse base current had to be known.

Fig. 5 shows a block diagram of the circuit used in the experiment. The base drive circuitry consists of regulated current sources that are variable in both amplitude and time. The voltage compliance of the current sources is limited to less than the emitter base avalanche voltage. This was done to be certain that I_{B2} did not contain an avalanche component of current. The base supplies can source or sink 0.1 to 10 A.

The collector circuit consists of a crowbar circuit, a detection circuit that can activate the crowbar, and an inductance to drive the device (Ldi/dt) into second breakdown. The collector current changes only a few percent during the test time even though the collector voltage may change up to 1000 volts. Since the collector voltage may change at a rate of 30 kV/μS, it is essential that the interwinding capacitance be minimized. A 800 μH inductor was used for the experiments.

The crowbar removes the collector current from the device at a given time after the initiation of second breakdown. This is done by applying a short across the collector-emitter terminals and shutting down the current source. The remaining stored energy in the inductor is dissipated through a set of fly back diodes connected across the inductor. The crowbar circuitry had to be very fast and also handle over 50A of current. For transistors used in this investigation, it was found that there was no degradation of the device if they were subject to second breakdown for less than 350 nS.

The input signal to trigger the crowbar can come from the detection circuit in the collector or from the crowbar synchronization circuit in the base. The detection circuit senses the rate of change of collector voltage (dv/dt) when the device comes out of saturation. The output signal from the detector has a fixed time constant and, if used to trigger the crowbar, takes 350 nS from the detection to the clamping of the collector current. If the crowbar synchronization is used, the time the device is in second breakdown can be varied. The transition from I_{B1} to I_{B2} starts a timing circuit that is adjustable from 1-15 μS. The output of the timer is then used to activate the crowbar.

The test procedure involved in using this circuit to observe a second breakdown is quite simple. Knowing the dc resistance of the main inductor and an approximate value for the saturation voltage of the device allows one to set the collector dc supply voltage in order to test at the desired value of collector current. Test values of the forward and reverse base current amplitudes are set with two potentiometers. The L/R time constant of the main inductor is required to set the length of the forward base current pulse so that the collector current will reach its nominal test value before the reverse base current is applied. The desired time durations of the forward and reverse base current pulses are then set with a combination of switches and potentiometers. After choosing the mode of crowbar shutdown and resetting the crowbar control circuitry following the previous test, a pushbutton then initiates the entire test sequence.

Limitations of the circuit are the following: The collector node capacitance to ground limits the dv/dt and allows a variation in the collector current. This capacitance is about 50 pf and fortunately does not affect the collector current by more than a few percent. The capacitance associated with the base node is about 0.01 μf. Because of the lower dv/dt at the base terminal, this does not present a problem.

The test equipment used for measuring the input and output parameters consisted of two current probes, a storage oscilloscope, and a high voltage probe. The current probes have a risetime of 7.5 nS and measure up to 10 A. The bandwidth of the oscilloscope is 100 MHz and that of the high voltage probe is 120 MHz. As the experiment involved very fast switching, the total system risetime had to be determined. This was done as follows:

$$\tau_r = \left(\tau_s^2 + \tau_p^2\right)^{1/2} = 8.3 \text{ nS}$$

where τ_r = system risetime, τ_s = scope risetime (0.35/BW), and τ_p = current probe risetime. This shows that if the risetime of the current waveforms as measured on the oscilloscope is greater than four times the risetime of the system τ_r, the actual risetime of the pulse will be within three percent of the measured pulse. The risetime for the scope and probe is similarly calculated to be 4.5 nS. Because the extremely low value of falltime associated with the collector voltage is predicted by the avalanche initiation theory, a square wave generator was used to establish that the risetime of the probe and the oscilloscope was 5 nS. The extremely high magnitude of dv/dt associated with the collapse of the collector voltage results in a great deal of electromagnetic interference that made it very difficult to monitor the waveforms after second breakdown. The electromagnetic interference picked up by the probes could not be filtered out. As this problem occurred only after breakdown, it does not affect the measurements.

The oscillograph is Fig. 6a shows the two input and two output parameters. The values of the input parameters I_{B2} and I_C chosen for this trace were 1A and 10 A, respectively.

The output parameters V_{CE} and V_{BE} show the device went into reverse bias second breakdown at V_p = 790 V and at that time V_{BE} = 6 V. The very fast collapse of the collector voltage is shown clearly in Fig. 6b. This picture has better resolution because the oscilloscope was used in its higher writting speed. It may be seen that the falltime measures about 12 nS. This value along with the risetime of 5 nS for the

probe and oscilloscope gives a ratio of the measured time to the system time of 2.4. This indicates that the actual voltage pulse on the collector is about 7 percent faster.

The temperature effects on second breakdown were also studied. The oscillograph in Fig. 7 shows that as the device's temperature increases from 25° to 150° C in 25° C steps, the value of the second breakdown voltage increased from 650 V to 680 V.

When the electrical tests were completed, the transistors were taken off the heat sinks. The chips were mounted on stainless steel angled blocks, and the junctions bevelled to a known angle. The spreading resistance probe was used to accurately measure the impurity concentration as a function of junction depth. A typical profile of a transistor is shown in Fig. 2. The values of the emitter, base, and collector impurity concentrations and junction depths provide the inputs for the analytical solution of eqs. (1)-(8).

RESULTS

The results from both the analysis and experiment are summarized in Tables I and II. Excluded from these results is the excellent agreement between the calculated and measured values of the reverse biased emitter-base voltage. The range of these voltages was between 6 to 9 volts. As the typical BV_{EBO} for the devices studied was 15 to 16 volts, in no case was there avalanche breakdown of the emitter junction.

DISCUSSION

It is seen from Tables I and II that there is excellent agreement between calculated and measured values of second breakdown voltage V_p. The correlation is good even though there is a wide range of collector base breakdown voltages (650-1000 V) and collector currents (5 to 12 A). It was found that the current density was very sensitive to the base width, and, therefore, great accuracy was necessary in its determination. When one considers the number of variables that were necessary to calculate V_p, the remarkable agreement between theory and measurement can be ascribed to two factors. The first is that the validity of the assumptions made in the analysis have been borne out, and secondly, that the phenomena of avalanche injection is in fact the triggering mechanism for reverse biased second breakdown.

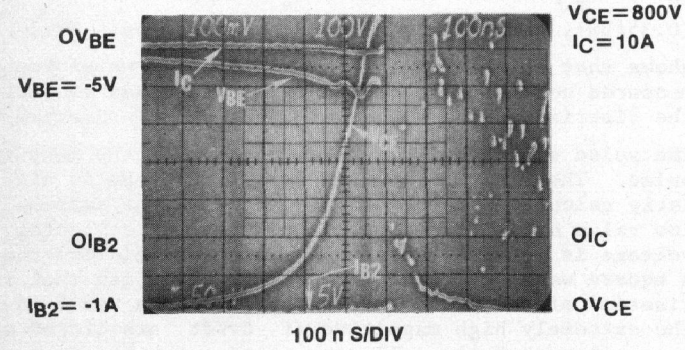

Fig. 6a Input and Output Parameters at Second Breakdown

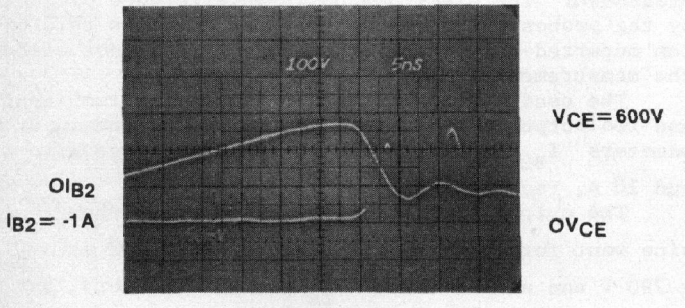

Fig. 6b Expanded Oscilloscope Sweep Showing the Fast Falltime of the Collector Voltage Associated with Reverse Bias Second Breakdown

It was shown in the experiment that although the collector current and the load inductance were held constant, V_p varies from one device to the next. Therefore, the rating of the transistors for second breakdown energy $1/2\ LI_C^2$ is clearly in error. The claim of Tasca's analysis [12] that $Et_d^{-1/2}$ is constant if the delay time is less than the thermal time constant may still be valid. This is because the stability of the current filament formed following avalanche injection may well be determined by this energy.

It seems appropriate at this point to ask the question: What is the difference between forward biased second breakdown? As far as a n^+-p-n$^-$-n^+ transistor is concerned, the collector junction supports a high voltage and conducts a high current. If breakdown occurs at this junction (and this is a reasonable assumption), there must be other factors influencing it. It is seen that in the experiment and calculations the emitter-base junction is at no time in breakdown, and, therefore, the reverse bias of the junction is not a determining factor. The only significant difference between the forward and reverse bias cases is that in the former the emitter (and collector) current density is much lower than in the latter. For the transistors in this study the maximum forward biased current density was 90 A/cm^2, and the reverse biased J_{max} varied from 670-800A/cm^2 for the same collector current of 10A. Further, it has been shown [4], [8] that in the forward biased case the entire collector-base junction region is at an elevated temperature that leads to thermal ionization, a lateral instability, and finally a runaway condition. A weak spot would result in a channel melt through. In the reverse bias case it is the local regions where avalanche breakdown occurs. This leads to the formation of filamentary currents and results in nucleation, and finally melt through. It has been observed [15] that when the lateral base current is increased to the point where it is equal to the collector current, i.e., the emitter is effectively disconnected, the threshold for reverse bias second breakdown is substantially increased. In this situation there cannot exist a high "pinched in" current density (because $I_E = 0$) and, therefore, there is no observable reverse bias breakdown. It would be safe to assume that if the base collector diode current was increased, there would be a point reached where second breakdown would occur due to thermal effects. It is commonly understood that the threshold for forward biased second breakdown is substantially reduced with increasing junction temperature. This would be expected of a thermal mechanism. However, as seen in Fig. 7, there is an increase in the threshold for second breakdown V_p in these experiments. This is further evidence that the thermal effects are not the responsible factors.

Finally, one must attempt to put into perspective the relative merits of the thermal ionization theory as suggested by Sunshine et al. [13], Smith et al. [14] and the avalanche injection theories suggested by Thornton et al. [1] and Hower et al. [6]. While there is no disagreement that the failure mode is due to a melt through caused by high temperatures, the equation remains as to what is the triggering mechanism. It is interesting to note that Smith et al. worked with Silicon on Sapphire (SOS) diodes at extremely high current

densities of the order of 4×10^4 A/cm^2, where the avalanche effects would certainly be present. However, the observations that were made were to detect heat. It would seem incongruous to expect, therefore, the detection of avalanche multiplication, but rather its effect, once triggering has been completed. Again it should be pointed out that the basic causes given by others [13], [14] is the increase in generation and saturation currents. High temperatures should, therefore, greatly influence the saturation current and lower the second breakdown potential. However, this is not observed; quite the contrary situation occurs and is shown in Fig. 7. The observations by Sunshine et al. [13] and others are certainly relevant. Failure due to reverse bias second breakdown may encompass both the avalanche and the thermal initiation processes in the following sequence:

Base current flows out, pinching in the emitter current density. The increase in space charge produced in the presence of high voltage triggers localized avalanche breakdown. The resulting carriers form stable current filaments by the balancing out of the electric field force and the diffusion gradient. These filaments grow and are ballasted by the high resistivity of the collector which provides a large spreading resistance. Further increase in the filament growth leads to a melt through of the junction and n^- region. The high temperature of the molten silicon provides a low conductivity path between the base and collector, and the voltage drops precipitously. This scenario is attractive because it is simple and reconciles most of the experimental observations of others to the theoretical and experimental evidence in this paper.

APPENDIX

Derivation of the Lateral Base Conductivity

The equations for electron and hole current flow are shown below

$$J_n = q\mu_n n(x)E + qD_n \frac{dn(x)}{dx} \tag{A1}$$

$$J_p = q\mu_p p(x)E - qD_p \frac{dp(x)}{dx} \tag{A2}$$

Under the high injection conditions almost always present, i.e., $n_e(x) = n_i \exp qV(x)/2kT$, the lateral electron and hole base currents are given as

$$J_{bn} = \frac{1}{2} q\mu_n n(x)E \tag{A3}$$

$$J_{bp} = \frac{3}{2} q\mu_p n(x)E + q\mu_p N_a E \tag{A4}$$

where N_a is the acceptor concentration and $p(x) = n(x) + N_a$. Thus, the total value of the base current is

$$J_b = \left(\frac{1}{2}\mu_n + \frac{3}{2}\mu_p\right) qn(x)E + q\mu_p N_a E \tag{A5}$$

As can be seen, the lateral base conductivity is composed of two parts as indicated earlier in the main text. There is a constant part and a part due to carrier modulation effects. In the following we will further consider this modulated part.

The value of the electron concentration varies both laterally and vertically through the base region. The lateral variation is explicitly included in the equation for the lateral base current (eq. (A5)), but to include the vertical variation, an average of the electron concentration through the base must be performed. Since we are calculating a conductivity to be used in determining the lateral voltage drop in the base, the average should be weighted in favor of the regions of the base where most of the carriers are present. If the electron concentration is used as the weighting factor and its spatial dependence is given as $n(x,y) = n_e(x)(1 - y/W_B)$, where $n_e(x)$ is the concentration at the emitter-base junction and W_B is the base width, the average base conductivity is given as

$$\sigma_1(x) = q\left(\frac{1}{2}\mu_n + \frac{3}{2}\mu_p\right) n_e(x) \frac{\int_0^{W_B} \left(1 - \frac{y}{W_B}\right)^2 dy}{\int_0^{W_B} 1 - \frac{y}{W_B}\, dy} \tag{A6}$$

thus,

$$\sigma_1(x) = \frac{2}{3} q\left(\frac{1}{2}\mu_n + \frac{3}{2}\mu_p\right) n_e(x) \tag{A7}$$

This essentially completes the derivation of eq. (3) in the main text where it is now seen that the effective mobility is given as

$$\mu_{eff} = \frac{1}{2}\mu_n + \frac{3}{2}\mu_p$$

It only remains to evaluated μ_{eff} for the specific conditions encountered in the experimental measurements. In doing this, allowance was made for the scattering from ionized impurities and mobile carriers. Mobile carriers and impurities were treated alike and values of 10^{17} cm^{-3} holes, 6×10^{16} cm^{-3} electrons, and 4×10^{16} impurities were in general present at the center of the base at the base-emitter junction. This gives a total of 2×10^{17} cm^{-3} scattering centers at this point. In order to obtain the average number of scattering centers in the base, a weighted average over the vertical dimension, as above, and a straight average over the lateral dimension were taken. This re-

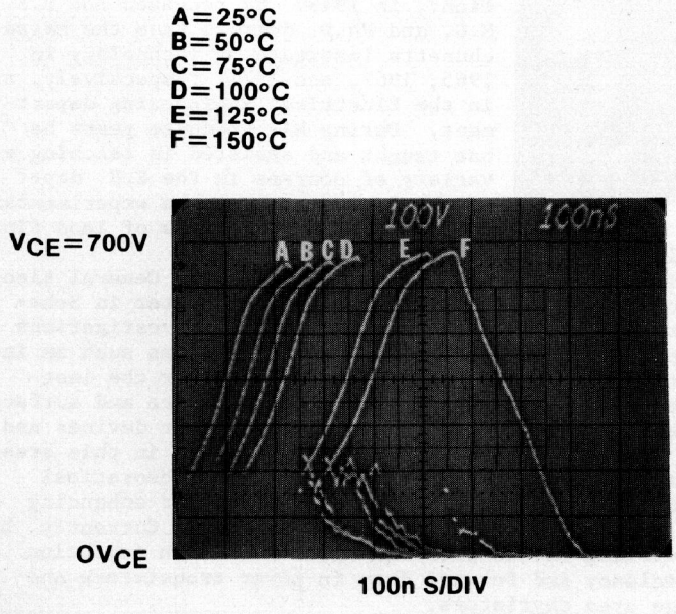

Fig. 7 Second Breakdown Voltage V_p Versus Temperature

sults in an average of 6.7×10^{16} cm^{-3} scattering centers. Using tables in Sze [19] as a source, this results in values of 800 for μ_n and 380 for μ_p.

ACKNOWLEDGMENTS

The authors are greatly indebted to Dr. P. V. Gray for his assistance in the numerical solution in this study. His general consultation is also appreciated. We would also like to thank Mr. M. L. Torreno for his assistance in the fabrication of the devices and Miss C. O. Davies for typing the manuscript. This work was a partial fulfillment toward the MS degree for B. Beatty.

REFERENCES

[1] C. G. Thornton and C. D. Simmons, "A New High Current Mode of Transistor Operation," IRE Trans. Electron Devices, Vol. ED-5, January 1958.

[2] H. B. Grutchfield and T. J. Moutoux, "Current Mode Second Breakdown in Epitaxial Planar Transistors," IEEE Trans. Electron Devices, Vol. ED-13, November 1966.

[3] H. A. Schefft, "Second Breakdown - A comprehensive Review," IEEE Proc., Vol. 55, August 1967.

[4] R. M. Scarlett and W. Shockley, "Secondary Breakdown and Hot Spots in Power Transistors," IEEE Int. Conv. Record, part 3, 1963.

[5] S. P. Gaur, D. H. Navon, and R. W. Teerlink, "Transistor Design and Thermal Stability," IEEE Trans. Electron Devices, Vol. ED-20, June 1973.

[6] P. L. Hower and V. G. K. Reddi, "Avalanche Injection and Second Breakdown in Transistors," IEEE Trans. Electron Devices, Vol. ED-17, April 1970.

[7] S. Krishna and P. L. Hower, "Second Breakdown of Transistors during Inductive Turn Off," IEEE Proc. Vol. 61, March 1973.

[8] S. Krishna and P. V. Gray, "Second Breakdown: Hot Spots or Hot Cylinders," IEEE Proc., Vol. 62, August 1974.

[9] F. Bergmann and D. Gerstner, "Thermisch Bedingte Stromein-Schnu rung Bei Hochfrequenz-Leistungstransistoren (Ein Beitreg zum Problem des Second Breakdown)," Arch Eleckt Ubertragung, Vol. 17, October 1963.

[10] H. Melchior and M. J. O. Strutt, "Secondary Breakdown in Transistors," Proc. IEEE, Vol. 52, April 1964.

[11] A. C. English and H. M. Power, "Mesoplasma Breakdown in Silicon Junctions," Proc. IEEE, Vol. 51, March 1963.

[12] D. M. Tasca, "Pulse Power Failure Modes in Semiconductors," IEEE Trans. Nuc. Sci., Vol. NS-17, December 1970.

[13] R. A. Sunshine and M. A. Lampert, "Second Breakdown Phenomena in Avalanching Silicon-on-sapphire Diodes," IEEE Trans. Electron Devices, Vol. ED-19, July 1972.

[14] W. B. Smith, D. H. Pontius, and P. P. Bundenstein, "Second Breakdown and Damage in Junction Devices," IEEE Trans. Electron Devices, Vol. ED-20, August 1973.

[15] T. M. Jahns, "Investigation of Reverse Bias Second Breakdown in Power Transistors," M.S. Thesis, M.I.T., May 1974.

[16] L. A. Hahn, "The Saturation Characteristics of High Voltage Transistors," Proc. IEEE, Vol. 55, pp. 1384-1388, August 1967.

[17] JEDEC Suggested Standard on Power Transistors, "Safe Operating Conditions for Power Transistors," part 3 of JC-25, May 1973.

[18] R. Van Overstraeten and H. DeMan, Solid State Electron, Vol. 13, pp. 583-608, (1970).

[19] S. M. Sze, Physics of Semiconductor Devices, John Wiley and Sons, New York, p. 40 (1969).

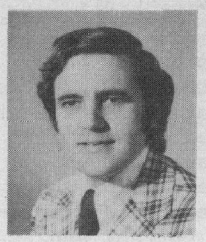

Brent A. Beatty was born in Detroit, Mich., on January 16, 1941. He received the A.A.S. degree in electrical engineering from DeVry Technical Institute, Chicago, Ill. in 1962, and the B.S. and M.S. degrees in electrical engineering from Union College, Schenectady, N. Y., in 1973 and 1976, respectively.

In 1962, he joined Sperry Flight Systems Division, Ariz., where he investigated failure mechanisms in solid-state devices in their failure analysis laboratory. In 1970, he joined the General Electric Corporate Research and Development Center, Schenectady, N. Y., where he was engaged in the circuit design and analysis of light activated circuits. Since 1973, he has been responsible for the design of power transistors and their final testing.

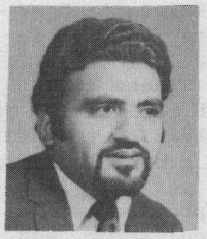

Surinder Krishna was born in Burma on September 4, 1940. He received the B.Sc. degree in physics from Calcutta University in 1958, the B.Sc. in electrical engineering, and a first class B.Sc. Houours in electrical engineering in 1962 and 1963 from the University of Edinburgh, Scotland. He was the recipient of the Edinburgh University awards in Electronics and Communications.

From 1963 to 1964 he was associated with Chelmsford, England. In 1964, he joined the Amperex Electronic Corporation in Cranston, R. I. and was responsible for the design and development of microwave power transistors. In 1967, he joined the Westinghouse Electric Corporation, first at the Semiconductor Division, Youngwood, Pa., and later at the Research and Development Center, Pittsburgh, Pa. His primary areas of study were the physics and technology of bipolar power transistors, thyristors, microwave field effect transistors, and Impatt diodes. In 1972 he joined the Corporate Research and Development Center, General Electric Company, and served from 1973 to 1975 as Manager of the Power Devices Unit. Presently he is engaged in the study and development of high frequency power semiconductor devices.

He is the author of several papers, recipient of an Industrial Research (IR-100) Award in 1976, and has received 12 patents covering his inventions.

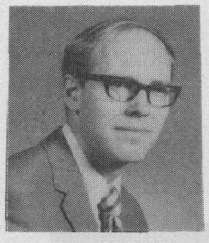

Michael S. Adler was born in Detroit, Mich., in 1943. He received the B.S., M.S. and Ph.D. degrees from the Massachusetts Institute of Technology in 1965, 1967, and 1971, respectively, all in the Electrical Engineering department. During his graduate years he has taught and assisted in teaching a variety of courses in the E.E. dept. His Ph.D. research was an experimental and theoretical study of the ban structure of lead tin telluride.

Since 1971 he has been employed at the General Electric Company Research and Development Center in Schenectady, N.Y. He has done theoretical investigations on a variety of practical physical problems such as induction heating and light scattering. For the last three years he has been working on a device and surface physics unique to high power semiconductor devices and has written and presented numerous papers in this area. This work has included experimental and theoretical studies of new and existing approaches for enhancing the break-down voltage in power devices. Currently, he is working on the problems associated with injection efficiency and forward drop in power transistors and large area thyristors.

Dr. Adler is a member of the ETA KAPPA NU and SIGMA XI.